Published OnlineFirst August 6, 2019; DOI: 10.1158/0008-5472.CAN-18-3712

Tumor Biology and Immunology

Cancer Research

The Goldilocks Window of Personalized Chemotherapy: Getting the Immune Response Just Right

Derek S. Park[1,2], Mark Robertson-Tessi[2], Kimberly A. Luddy[3,4], Philip K. Maini[5], Michael B. Bonsall[1], Robert A. Gatenby[2,6], and Alexander R.A. Anderson[2]

Abstract

The immune system is a robust and often untapped accomplice of many standard cancer therapies. A majority of tumors exist in a state of immune tolerance where the patient's immune system has become insensitive to the cancer cells. Because of its lymphodepleting effects, chemotherapy has the potential to break this tolerance. To investigate this, we created a mathematical modeling framework of tumor-immune dynamics. Our results suggest that optimal chemotherapy scheduling must balance two opposing objectives: maximizing tumor reduction while preserving patient immune function. Successful treatment requires therapy to operate in a "Goldilocks Window" where patient immune health is not overly compromised. By keeping therapy "just right," we show that the synergistic effects of immune activation and chemotherapy can maximize tumor reduction and control.

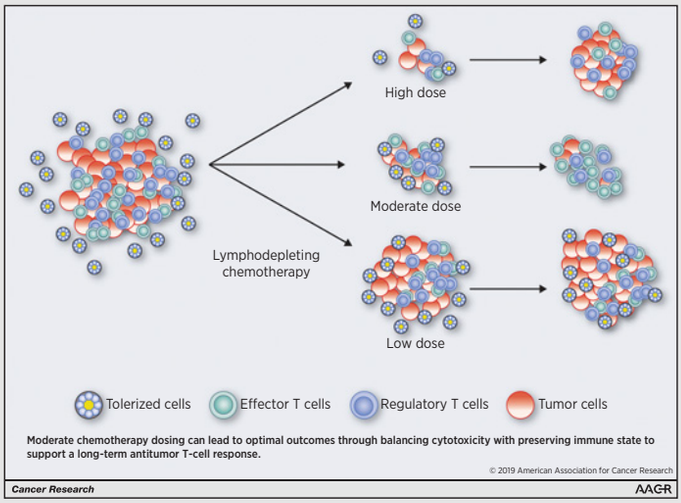

Significance: To maximize the synergy between chemotherapy and antitumor immune response, lymphodepleting therapy must be balanced in a "Goldilocks Window" of optimal dosing.

Graphical Abstract: http://cancerres.aacrjournals.org/content/canres/79/20/5302/F1.large.jpg.

Introduction

Immune tolerance occurs when the immune system fails to respond to a target despite its potential to induce an immune response. In cancer, this failure leads to immune evasion and tumor growth. $CD8^+$ effector T cells, also known as cytotoxic T lymphocytes (CTL), are an essential component of the adaptive immune system capable of responding to tumor antigens and inducing cell death. Immunologically inert tumors induce T-cell tolerance through multiple direct mechanisms such as inhibition of programmed death ligand 1 (PD-L1), activation of the T-cell regulatory protein CTLA4, and production of regulatory cytokines and metabolites (1), as well as indirect methods such as recruitment of regulatory T cells (Treg), myeloid-derived suppressor cells (MDSC), and tolerogenic dendritic cells (DC; ref. 2) Tregs inhibit CTL cytotoxic activity via cell-cell contact (3, 4) and through secreted factors such as TGFβ (5, 6). They have posed challenges for cancer immunotherapies as well as preventing the activation of the immune system during more traditional therapy approaches (4, 7).

Breaking tolerance requires removal of multiple suppressive factors and activation of cytotoxic immune cells. Chemotherapy, while toxic to CTLs, also has paradoxical and important immunostimulatory effects through dysregulation of the immunosuppressive tumor microenvironment by reducing regulatory cytokine levels, changes in oxygen levels, and reduced metabolites. Several chemotherapies, including cyclophosphamide, paclitaxel,

[1]Department of Zoology, University of Oxford, Oxford, United Kingdom. [2]Department of Integrated Mathematical Oncology, H. Lee Moffitt Cancer Center and Research Institute, Tampa, Florida. [3]Comparative Immunology Group, School of Biochemistry and Immunology, Trinity College Dublin, Dublin, Ireland. [4]Department of Cancer Physiology, H. Lee Moffitt Cancer Center and Research Institute, Tampa, Florida. [5]Mathematical Institute, University of Oxford, Oxford, Oxfordshire, United Kingdom. [6]Department of Radiology, H. Lee Moffitt Cancer Center and Research Institute, Tampa, Florida.

Note: Supplementary data for this article are available at Cancer Research Online (http://cancerres.aacrjournals.org/).

Corresponding Authors: Derek S. Park and Alexander R.A. Anderson, Department of Integrated Mathematical Oncology, H. Lee Moffitt Cancer Center and Research Institute, 12902 USF Magnolia Drive, Mailstop: SRB 4, Tampa, FL 33612. Phone: 813-745-6119; Fax: 813-745-8357; E-mail: Derek.park@aya.yale.edu; Alexander.anderson@moffitt.org

Cancer Res 2019;79:5302–15

doi: 10.1158/0008-5472.CAN-18-3712

Published OnlineFirst August 6, 2019; DOI: 10.1158/0008-5472.CAN-18-3712

gemcitabine, and 5-fluorouracil, can selectively target MDSCs and Tregs (8, 9).

In addition, highly cytotoxic chemotherapies with lymphodepleting effects create immunologic space (10, 11). During homeostasis, the body maintains T-cell pools at consistent levels. When these pools are depleted, T cells refill this space through antigen-independent proliferation, termed homeostatic repopulation, which favors memory T cells (12). This homeostatic proliferation breaks tolerance, temporarily restoring immune response to previously tolerated antigens (13). This was first characterized in the posttransplant setting where memory T cells lose peripheral tolerance during homeostatic repopulation, leading to graft rejection (12).

Chemotherapy-induced tolerance breaking is dynamic and transient, often requiring treatment breaks to achieve full effect. Various studies report that regulatory cells return 5–10 days post-treatment (8). Homeostatic repopulation following moderate lymphopenia can fully restore the lymphocyte pool as early as 4 days following therapy in murine models (14). Even in the case of nearly complete lymphodepletion using alemtuzumab in nonhuman primate transplant models, the T-cell pool is completely restored in 8 weeks, consisting of 96% memory T cells (15). An obvious question then arises: is there an optimal chemotherapy schedule that could maximize tumor kill and also enhance immune response?

To investigate this question, we created a mathematical model of the complex tumor-immune dynamics that occur during multiple cycles of chemotherapy. In particular, we investigated three, clinically relevant, therapeutic dynamics: immunodepletion, immunostimulation via vaccination, and

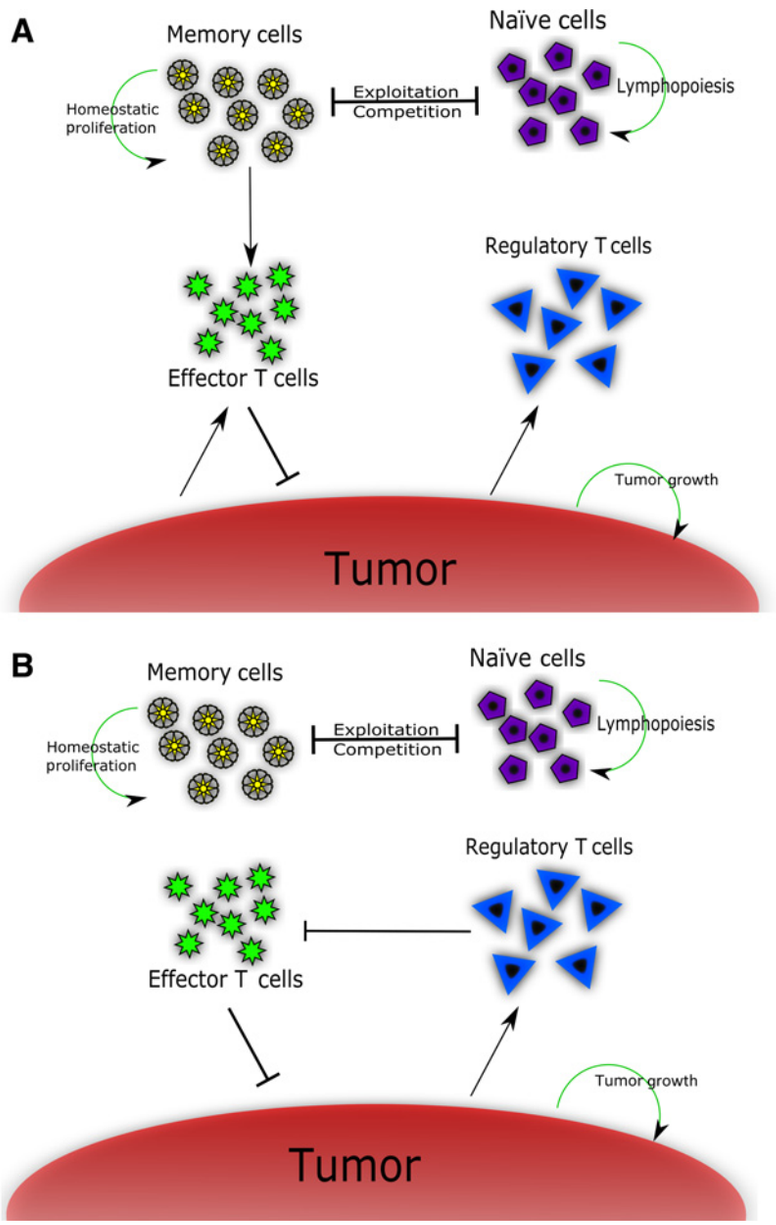

Figure 1.
Tumor-immune dynamics during the sensitive (**A**) and tolerant (**B**) stages of the immune response. During antigen-sensitive immune expansion, CTLs are recruited from memory cells to attack tumor cells. Tregs are being recruited but have not yet started significantly inhibiting CTL responses. During immune contraction once tolerance sets in, Tregs exert an active inhibitory pressure on CTLs. Expansion of memory cells into CTLs ceases. Both stages of the immune response are characterized by competition between memory and naïve immune cells for common cytokine pools as well as homeostatic proliferation and lymphopoiesis.

Published OnlineFirst August 6, 2019; DOI: 10.1158/0008-5472.CAN-18-3712

immunosupportive prophylactics. We identified significant immune trade-offs during chemotherapy as well as the relevant patient metrics that determine the magnitude and severity of these compromises. Furthermore, by exploring the impact of clinically-established therapy, as well as more experimental treatment decisions, we illustrate a more complex interplay between chemotherapy and patient immune dynamics than has been previously investigated. Our results indicate that optimal chemotherapy requires identification of a "Goldilocks Window" in which treatment can both induce cytotoxic effects in the tumor and enhance the immune response to tumor antigens. Therefore, instead of the one-size-fits-all paradigm of fixed therapy regimens, patient immune biology should be a key consideration when developing personalized chemotherapy strategies.

Materials and Methods

Overall model design

A central assumption of this work is that a clinically detectable tumor has induced a tolerant state in which the immune system can no longer respond to tumor antigens. Chemotherapy temporarily removes this tolerance through lymphodepletion, which eliminates Tregs and allows a burst of immune response. However, the lymphodepletion itself also kills CTLs and therefore reduces the potential cytotoxic efficacy. This double-edged response to chemotherapy implies that there is an optimal therapeutic strategy.

We develop a mathematical model that includes five major populations of cells: tumor cells (T), CTLs (E), Tregs (R), memory T cells (M), and naïve T cells (N). Immune function is separated into two distinct temporal stages, relative to the time of application of each chemotherapy cycle: (i) a period of CTL expansion immediately following the application of chemotherapy (Fig. 1A); and (ii) CTL contraction as tolerance returns (Fig. 1B). The transition time between these phases remains poorly characterized, but empirically occurs 5–10 days after the expansion starts (16). This range has been observed in murine models and is dramatic, involving over a 90% decrease in population size (17). A central assumption of this work is that a clinically detectable tumor has induced a tolerant state in which the immune system can no longer respond to tumor antigens. Systemic lymphodepletion, including that caused by chemotherapy, can help break this tolerance. This can have drastically different effects depending on the type and strength of lymphodepletion (18, 19). First, chemotherapy can selectively reduce Tregs (20, 21, 22) helping to break peripheral tolerance. Second, strong lymphodepletion will cause homeostatic proliferation in the lymphoid compartment, further reducing tolerance.

However, dead immune cells cannot elicit cytotoxic effects or engage in homeostatic proliferation. This implies that there is an optimal therapeutic strategy. If the dose is too high, then the few remaining immune cells will not be able to take advantage of the tolerance breaking; if the dose is too low, then the lymphodepleting effects will be insufficient to break tolerance. In addition to these immune effects, the chemotherapy itself can induce cancer cell death affecting both the tumor size directly and releasing tumor antigens, adding another layer of complexity to the tumor-immune dynamics.

While the full course of lymphocyte recoveries are not observed in the treatment course, measurements of lymphocyte populations over time have shown that a stable equilibrium is reached between chemotherapeutic depletion and population sizes (23). Therefore, in the model, there is a window of 5 days immediately following each chemotherapy cycle in which the immune system is sensitive, and outside of these periods, it is tolerant. We explore the length of this window more thoroughly below.

Our efforts to use mathematical modeling to inform chemotherapy build upon previous immune and personalized medicine works. Mathematical models of tumor-immune activity are numerous, given the complexity of the mechanisms involved (see refs. 24–28) for examples relevant to the current work). Explained more fully below, we extend the modeling work of Robertson-Tessi and colleagues (29) to a more clinically oriented setting by simplifying the immunosuppressive dynamics while maintaining Treg recruitment and function. There have been efforts to study explicit spatial dynamics of the growing cancer cell population in the context of healthy tissue (30, 31). Here, we implement an implicit spatial limitation on growth (see explanation of $f(T)$ below); our model may be extended in the future to incorporate explicit spatial dynamics. Our initial framework choices have been to incorporate patient immune parameters to build toward a model for personalized oncology (32).

During the phase in which the immune system is sensitive to the tumor, a few key processes occur. CTLs, which target and kill the tumor, are recruited from a memory cell population due to response to tumor antigens (16). Recent studies indicate that memory T cells make up the majority of T cells engaged in homeostatic repopulation (15, 33). These memory cells are constantly undergoing a low level of replenishing proliferation, but they only convert to CTLs during the sensitive expansion phase following lymphodepletion. During this phase, there is also tumor-mediated recruitment of Tregs. This eventually causes a significant shift in immune dynamics, leading to a contraction of the CTL compartment during the tolerized phase. Under tolerance, there is no longer a significant recruitment of CTLs from the memory cell compartment. Instead, while the existing CTLs do carry out some tumor-killing function, the Tregs decrease the CTL number.

Quick guide to equations and assumptions

$$\frac{dT}{dt} = \frac{T}{f(T)} - k_0 \frac{TE}{T+E}\left(1 - b\frac{R}{R+E}\right)$$

$$f(T) = \left(\left(\frac{1}{T_{trans}^{m-1} r_T}\right)^p + \left(\frac{T^{1-m}}{r_T}\right)^p\right)^{\frac{1}{p}}$$

$$\frac{dE}{dt} = H(t_{off} - t)\left(1 - \frac{M+N}{K_{max}}\right)\gamma\alpha\frac{TM}{T+M} - H(t - t_{off})\left(\rho E\left(1 + c\frac{R}{R+E}\right) + \delta_E E\right)$$

$$\frac{dM}{dt} = r_M M\left(1 - \frac{M+N}{K_{max}}\right) - H(t_{off} - t)\left(1 - \frac{M+N}{K_{max}}\right)\alpha\frac{TM}{T+M} + H(t - t_{off})\rho\omega E$$

$$\frac{dR}{dt} = \sigma T - \delta_R R$$

$$\frac{dN}{dt} = r_N N\left(\frac{1 - M + N}{K_{max}}\right)$$

Our immune tolerance model assumes that the growth of tumor cells (T) can be checked by CTLs (E). However, CTLs are

Published OnlineFirst August 6, 2019; DOI: 10.1158/0008-5472.CAN-18-3712

themselves inhibited by Tregs (R) that are recruited at a rate σ by tumor antigens. This leads to CTL-mediated tumor cell death being moderated by the quantity of Tregs ($\frac{R}{R+E}$). CTLs exhibit different behaviors during immune expansion and immune contraction. This switching behavior is modeled with the Heaviside function ($H(t_{off}-t)$). During the immune expansion phase, CTLs are recruited from the memory pool based on both available memory cells (M) and the tumor burden ($\frac{TM}{T+M}$). During immune expansion, the antigenicity of the tumor (α) induces differentiation to CTLs ($\frac{TM}{T+M}$). However, as immune tolerance sets in, there is a contraction in the CTL population, caused by degradation of CTLs by Tregs (b). During immune contraction, CTLs can convert back to memory T cells ($\omega E,\ \omega<1$). Finally, the total remaining lymphocyte population that is not sensitive to the tumor (N) replicates in a logistic growth model $r_N N(1-\frac{M+N}{K_{max}})$.

Tumor dynamics

$$\frac{dT}{dt}=\underbrace{\frac{T}{f(T)}}_{1}\underbrace{-k_0\frac{TE}{T+E}\left(1-b\frac{R}{R+E}\right)}_{2} \tag{A}$$

Tumor growth dynamics (term 1) are approximated via a combination of exponential growth for smaller tumors and power law growth for larger tumors. This growth model includes a few key assumptions about the limitations that a growing tumor faces before clinical detection. In the absence of effector cells attacking the tumor population, tumor cells first grow exponentially but then transition to power-law growth. This growth dynamic is typical of early-stage, preclinical malignant growths and is based on mathematical modeling as well as experimental observation (29). Furthermore, there are also practical limitations to the biological validity of the tumor population sizes that the model can approximate. While the model can simulate unbounded tumor growth, this is obviously clinically impossible due to the resulting morbidity and eventual patient mortality. Here, we restrict the analysis to the range of tumor sizes that are typical for clinically detectable masses, namely $T<10^{10}$ cells. The transition between exponential and power law growth dynamics is governed by $f(T)$ as defined in Eq. B.

$$f(T)=\left(\left(\frac{1}{T_{trans}^{m-1}r_T}\right)^P+\left(\frac{T^{1-m}}{r_T}\right)^P\right)^{\frac{1}{P}} \tag{B}$$

The function $f(T)$ employs the method of modeling tumor growth in ref. 29. Beyond a certain size (T_{trans}), small tumors are not able to sustain their early exponential growth due to physical and nutrient limitations, and therefore transition to power law growth at larger tumor sizes. The smoothness of this transition is governed by the exponent P. The parameter r_T represents the tumor growth coefficient.

Term 2 of Eq. A represents the tumor loss due to killing by CTLs. Parameter k_0 represents the CTL cytotoxic efficacy, with the actual tumor kill rate dependent upon the relative numbers of tumor and CTLs ($\frac{TE}{T+E}$). An estimate of this efficacy was initially set at 1 day^{-1} based on the potency of CTLs in preventing tumor growth when stimulated by multiple types of tumor antigen (34). *In vivo* killing capacities of CTLs have also been measured in the 1–10 day^{-1} range by real-time imaging in viral systems, although there is significant heterogeneity (35). However, this rate is mitigated by the presence of Tregs, with b representing their inhibition efficacy. As Tregs increase in density, the CTL-mediated tumor death rate decreases.

CTL dynamics

$$\frac{dE}{dt}=\underbrace{H(t_{off}-t)}_{1}\underbrace{\left(1-\frac{M+N}{K_{max}}\right)}_{2}\underbrace{\gamma\alpha\frac{TM}{T+M}}_{3}\underbrace{-H(t-t_{off})}_{4}\left(\underbrace{\rho E\left(1+c\frac{R}{R+E}\right)}_{5}+\underbrace{\delta_E E}_{6}\right) \tag{C}$$

CTL dynamics are modeled in two phases, expansion (terms 1–3) and contraction into tolerance (terms 4–6). Terms 1 and 4 switch between these phases via the Heaviside function, with t_{off} being the length of the expansion phase (5 days, unless noted) immediately following each round of chemotherapy. Terms 2 and 3 govern the growth of CTLs during immune sensitivity to the tumor. CTLs are generated based upon the antigenicity of the tumor (α) as well as the number of tumor and memory cells. Modulating this is an amplification rate, γ, since one memory cell can yield multiple CTLs. Term 2 accounts for the maximum number of lymphocytes that can be supported by the cytokine pool. This paradigm of CTL function being limited by cytokine availability is supported by lymphodepletion studies showing increased CTL activity when IL7 and IL15 cytokine-responsive cells were removed (36). When the immune compartment is full and in homeostasis, this term will be near zero, effectively shutting down CTL recruitment; however, immediately after a dose of chemotherapy, memory and naïve T cells are depleted, which promotes CTL expansion.

Term 5 represents the contraction of the CTL compartment that occurs due to immune tolerance. The death rate of CTLs during contraction, ρ, is due to decreases in the level of supportive cytokines. This rate is increased by the relative fraction of Tregs that are present, $\frac{R}{R+E}$. The modifying constant c represents the sensitivity of CTL suppression to Tregs through a variety of mechanisms (37). Finally, term 6 represents the rate of conversion of CTLs back into memory cells, an active mechanism during immune contraction (38, 39).

Memory T-cell dynamics

$$\frac{dM}{dt}=\underbrace{r_M M\left(1-\frac{M+N}{K_{max}}\right)}_{1}\underbrace{-H(t_{off}-t)}_{2}\underbrace{\left(1-\frac{M+N}{K_{max}}\right)}_{3}\underbrace{\alpha\frac{TM}{T+M}}_{4}+\underbrace{H(t-t_{off})}_{5}\underbrace{\rho\omega E}_{6} \tag{D}$$

Memory cells continually replenish themselves through homeostatic growth in term 1. Parameter r_M is the maximum memory cell growth rate, subject to a carrying capacity, K_{max}. During the immune expansion phase (terms 2–4), memory cells convert to CTLs, governed by the relative abundances of tumor and memory cells, $\frac{TM}{T+M}$, as well as the antigenicity (α). As described in Eq. C, the rate of recruitment is moderated by the homeostatic fraction of the overall immune system (term 3). During the contraction phase (terms 5 and 6), memory cells are replenished from the CTL compartment. A fraction (ω) of the CTLs is successfully converted back to memory cells (38). Because of some loss and inefficiency in conversion, $\omega<1$ (40).

Published OnlineFirst August 6, 2019; DOI: 10.1158/0008-5472.CAN-18-3712

Treg and naïve T-cell dynamics

$$\frac{dR}{dt} = \sigma T - \delta_R R \quad \text{(E)}$$

Tregs are recruited by tumor cells with rate $\boldsymbol{\sigma}$, and they decay with a rate $\boldsymbol{\delta_R}$ (41, 42).

$$\frac{dN}{dt} = r_N N\left(1 - \frac{M+N}{K_{\max}}\right) \quad \text{(F)}$$

Naïve T-cell dynamics follow homeostatic proliferation with rate $\boldsymbol{r_N}$, up to a common carrying capacity of $\boldsymbol{K_{max}}$, which is the maximum number of memory and naïve T cells in the immune system (43).

The model was parameterized on the basis of literature sources when possible, as shown in Table 1. For many cases, there was evidence of variation in parameters, and some cannot be easily measured. Where possible, we have tried to make a biologically reasonable order-of-magnitude approximation. To address this parameter uncertainty, we explicitly consider the impact of parameter variation on model results.

Simulating chemotherapy and evaluating outcomes

To establish tolerance in the system and allow transients from initial conditions to dampen before applying therapy, the simulation was initialized with a tumor size of 10^7 cells. Chemotherapy was started when the tumor reached 10^8 cells and was simulated as periodic doses of cytotoxic therapy at 14-day intervals. In total, 10 cycles of chemotherapy were applied. At the time of each treatment cycle, all cell populations (immune and tumor) were instantaneously reduced by a fraction $\boldsymbol{C_0}$ representing the cytotoxic effect of chemotherapy on that population.

This instantaneous death fraction can be understood as lethal dose (LD) values with, for example, $\boldsymbol{C_0 = 0.5}$ representing LD_{50}. The choice for an instantaneous decrease is simplifying, allowing us to omit pharmacodynamics; however, this approach reflects the general potency of many therapy agents. For example, *in vitro* studies have shown that cellular uptake and incorporation into RNA for 5-fluorouracil occurs as soon as 3 hours after exposure (44). Uptake levels were directly shown to correlate with cytotoxicity. For doxorubicin, cytotoxicity studies have found that just 1 hour of exposure is enough to induce a 90% decrease in viable, colony-forming cells (45).

Immune cells were reduced by the same fraction ($\boldsymbol{C_0}$) on each chemotherapy cycle. However, to account for tumor resistance to therapy, the fractional tumor reduction for cycle i ($\boldsymbol{C_i}$) was linearly reduced with each cycle, such that the cytotoxic fraction on the last cycle was 75% of the initial fraction $\boldsymbol{C_0}$. Approximating the impact of chemoresistance on drug efficacy is challenging since values vary for different classes of drugs. Furthermore, Hao and colleagues (46) noted dose-dependent differences of up to 400% between resistant and resensitized prostate cancer cell populations to docetaxel. Here, the value of 75% chemotherapy efficacy at the last cycle represents a 33% advantage of survivorship for a resistant population versus a susceptible population. It is a conservative estimate of the impact of resistance, but we believe it is reasonable given that tumor populations are unlikely to be entirely resistant. Varying this range is a relevant question for future research. For our purposes, $\boldsymbol{C_i}$ is given by:

$$C_i = C_0\left(1 - 0.25\frac{i}{10}\right) \quad \text{(G)}$$

The final tumor size after 10 cycles of chemotherapy was compared with the tumor size at the start of treatment (10^8 cells) and evaluated according to RECIST categories. Specifically, a total loss of tumor ($\leq$99% change in size) is a complete response (CR). A change between -30% and -99% is considered a partial response (PR). Tumor changes between -30% and $+20\%$ are classified as stable disease (SD) and increases of greater than $+20\%$ are seen as progressive disease (PD; ref. 47). While there are many different methods of measuring therapy efficacy impact on disease, RECIST categories were chosen here because they have correlated well with overall survival in patients across a variety of cancers.

Table 1. Model parameters were estimated based upon both preexisting models, chiefly Althaus and colleagues (16) and Robertson-Tessi and colleagues (29), as well as experimental studies

Parameter	Symbol	Value	Literature reference
Tumor growth coefficient	r_T	1,000 cells^{1-m} day^{-1}	29
CTL kill rate	k_0	1 day^{-1}	34, 35
Treg suppression efficacy	b	0.75	29
Tumor growth transition size	T_{trans}	10^6 cells	49
Power-Law growth exponent	m	0.5	29
Exponential to power smoothing term	P	3.0	29
Time till immune contraction	t_{off}	4–8 days	15
Maximum sustainable number of effector, naïve, and memory cells	E_{max}	10^{12} cells	40
Tumor antigenicity	α	1 day$^{-1,\,a}$	29
CTL death/apoptosis rate	δ_E	0.05 day$^{-1,\,a}$	39
CTL contraction rate	ρ	0.13 day^{-1}	15
CTL contraction augmentation due to Tregs	c	0.01[a]	29
Memory cell expansion factor	γ	100[a]	15, 48
Tumor-mediated Treg recruitment rate	σ	0.01 day^{-1}	42, 29
Treg death rate	δ_R	0.1 day$^{-1,\,a}$	29
Memory cell growth rate	r_M	0.01 day$^{-1,\,a}$	40
Memory cell reconversion rate	ω	0.01[a]	40
Naïve cell growth rate	r_N	0.1 day^{-1}	40
Maximum number of naïve T cells and memory cells	K_{max}	10^{12} cells	43
Baseline chemotherapy strength	C_0	Varied in simulation	

[a]For some parameters, the literature often indicated significant variation, so order-of-magnitude approximations were made. Similarly, certain parameters were not succinctly captured in literature studies and were therefore estimated. We have addressed the impact of potential parameter variation through sensitivity studies (see Results).

Simulation environment

The model was programmed in the Python language (ver. 2.7.11). The open-source packages Scipy (ver. 0.17.0), Numpy (ver. 1.10.4), and Matplotlib (ver. 1.5.1) were used for simulation of the ODEs as well as visualization of the results. The platform for the program was both an Intel Core i7-6820 HQ processor as well as the high performance computing cluster at H. Lee Moffitt Cancer Center and Research Institute (Tampa, FL). The source code is available at the github repository for the Integrated Mathematical Oncology department at github.com/MathOnco/Goldilocks.

Published OnlineFirst August 6, 2019; DOI: 10.1158/0008-5472.CAN-18-3712

Results

Patient memory cell populations determine a "Goldilocks Window" of optimal dosing

Memory cell population sizes are variable among patients (48). Arstila and colleagues have estimated 10^6–10^7 T-cell clones in the human body with approximately 10^5 memory T cells per antigen (48, 49). However, due to antigen responses being polyclonal, this suggests multiple orders of magnitude of potential variation in memory T-cell numbers. Therefore, varying doses of chemotherapy were simulated for a range of memory cell population sizes (Fig. 2A and B). Results from the model show that patient memory cell numbers significantly influence the optimum chemotherapy dose. Generally, there is a minimum memory cell population size that is necessary for any given strength of chemotherapy to be successful. Above this threshold, the more memory cells there are, the better the improvement with stronger doses of therapy. Conversely, this means that when memory cell populations are close to the minimum threshold, chemotherapy should be similarly weak for a more favorable outcome. Furthermore, if memory cells are below the minimum threshold, then the optimal strategy is to use strong chemotherapy (Fig. 2A and B), because the immune system will not contribute to tumor regression.

The double-edged nature of chemotherapy on the immune system can be better understood through the transient dynamics during therapy (Fig. 2C and D). In cases with stronger chemotherapy dosing, there is an early decrease in tumor population levels due to the cytotoxic strength of the therapy. However, we observe a trend that these strong therapies tend to lead to failure and larger final tumor sizes than if treated with a "weaker" chemotherapy regimen, which provides lower cytotoxicity on the tumor but maintain tumor size reduction for the duration of therapy.

This counterintuitive result stems from the fact that cytotoxicity alone is insufficient for suppressing tumor growth, especially due to the accumulating chemoresistance. Rather, it is the synergistic effect of cytotoxicity as well as the breaking of immune tolerance and consequent recruitment of CTLs that keeps tumor populations in check. Our *in silico* treatments consistently show that there is an inherent disadvantage to high-dose chemotherapy. There is a gradual decrease in the CTL population over multiple rounds of treatment due to the net loss that stronger dosing causes in memory T-cell populations (Fig. 2D). It is these memory cells that are affected the most by chemotherapy because they can only recover relatively slowly. If the cytotoxic pressure on memory cells is greater than the recovery rate of that compartment, then even with a resensitized immune system, expansion will lead to fewer total CTLs and ultimate treatment failure. In contrast, if the immunodepleting side effects of chemotherapy can be balanced with immune recovery, then more sustainable treatment responses are possible. In short, there is a tradeoff between having chemotherapy strong enough to sufficiently break tolerance, but

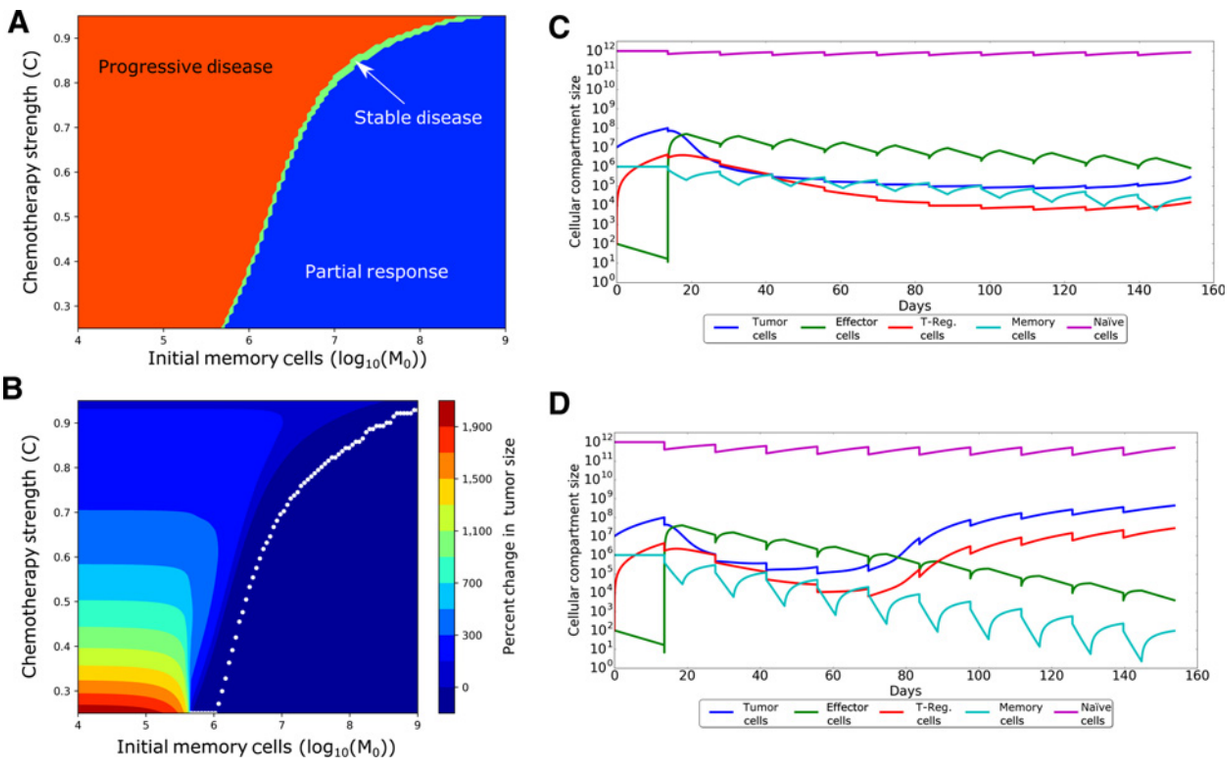

Figure 2.

Interaction of memory cell populations and chemotherapy strength on treatment outcomes. RECIST outcomes are shown in **A** with progressive disease (red), stable disease (yellow), partial response (light blue), and complete response (dark blue). **B,** Finer grade responses are shown as percent changes in tumor size after therapy versus the initial starting size (10^8 cells). The underlying dynamic reasons for these differences can be seen in the memory populations during low (**C**) and high-dose (**D**) chemotherapy. Low-dose chemotherapy allows memory populations (light blue) to be sustained for longer and generate larger CTL responses (green). High-dose chemotherapy, however, depletes memory cells faster and leads to declining CTL responses and concurrent tumor escape.

Published OnlineFirst August 6, 2019; DOI: 10.1158/0008-5472.CAN-18-3712

mild enough to leave sufficient memory T cells for adequate CTL expansion. Akin to the story of Goldilocks and the three bears, the balancing of these two immunologic goals leads to an intermediary chemotherapy strength that is "just right." *In silico* simulation shows that this "Goldilocks Window" is highly dependent upon patient-specific, preexisting memory T-cell populations.

Patient-specific tumor growth rate and immune strength determine chemotherapeutic flexibility

While we identified this Goldilocks Window of optimal, submaximal chemotherapy dosing, we also sought to explore it in the broader context of patient-specific disease and immune variation. For tumor growth rates, we found that successful treatment outcomes are more sensitive to chemotherapy dosing for faster growing tumors and less sensitive for slower growing tumors. Experimental and model analyses have shown that selection pressures on growing tumors can lead to significant heterogeneity in metabolism and growth rates (49) In our framework, the tumor growth rate parameter (r_T) was set to the maximum speed for doubling during the exponential growth phase (1,000 cells$^{0.5}$ day^{-1}, representing a doubling time of 1 day), but we also explored faster and slower growth rates (Fig. 3A and B).

In slower growing tumors (r_T < 1,000 cells$^{0.5}$ day^{-1}), chemotherapy's cytotoxic effects are sufficient for tumor control. After the partial tumor clearance due to each cycle, there is regrowth of the cancer cell population (Fig. 2A and B). For slower growing tumors, there is less intercycle regrowth and therefore cancer cell populations can be controlled by chemotherapy alone without the need for CTL killing. The result is that, for slower growing tumors, there is no Goldilocks Window.

However, for faster growing tumors (r_T > 1,000 cells$^{0.5}$ day^{-1}), it becomes necessary to maintain chemotherapeutic strength within the Goldilocks Window to achieve optimal outcomes. For these tumors, regrowth between chemotherapy doses is significant and demands the addition of CTL-mediated tumor killing for disease control. Chemotherapy that is stronger than the Goldilocks Window hamstrings the patient's immune activation.

Importantly, for the most aggressively growing tumors, there is actually a "worst case scenario" of intermediary chemotherapy strength (Fig. 3B). Here, the worst option for chemotherapy is not the strongest possible dose, but a "mid-range" strength in treatment instead. At this chemotherapeutic strength, the drug alone is insufficient to cause a reduction in tumor size. However, the dose is still strong enough to lead to severe memory cell depletion, undermining any immune efforts at constraining tumor growth.

Separate from tumor parameters, patient immune characteristics can also impact the sensitivity of treatment outcomes to chemotherapy dosing. One important parameter we sought to explore was the rate of CTLs in killing tumor cells (k_0, Fig. 3C and D). Without changing the initial patient memory cell populations ($M_0 = 10^6$ cells), or the tumor growth rate (r_T = 1,000 cells$^{0.5}$ day^{-1}), the CTL-mediated cytotoxicity rate was varied around the biologically realistic parameter of k_0 = 0.9 day^{-1} (34). CTL

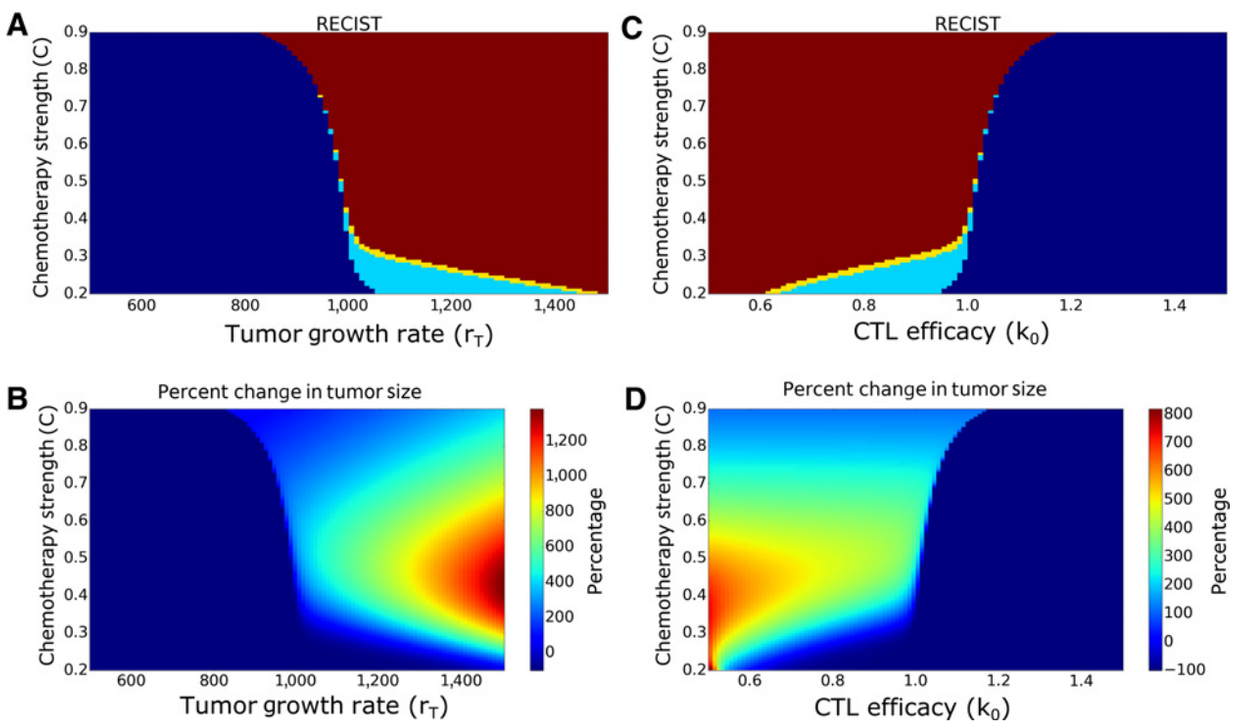

Figure 3.

Treatment outcomes for variation in tumor growth rate (**A** and **B**) and CTL efficacy (**C** and **D**). **A** and **C** represent RECIST outcomes. Red, progressive disease; dark blue, complete response; light blue, partial response; yellow, stable disease. Treatment outcomes with faster growing tumors are more sensitive to maintaining chemotherapy dosing in the Goldilocks Window. For slower growing tumors, treatment outcomes are more successful and less sensitive to dose. Similarly, more efficient patient CTLs lead to more successful outcomes and have less dependence on chemotherapy. However, outcomes become more sensitive to dosing for patients with less efficiently killing CTLs.

Published OnlineFirst August 6, 2019; DOI: 10.1158/0008-5472.CAN-18-3712

efficacy was found to dramatically impact sensitivity chemotherapy dosing and the Goldilocks Window. Lower rates of CTL-mediated tumor cell death lead to greater sensitivity of treatment outcomes on chemotherapy dosing (Fig. 2C and D). With a lower value of k_0, more CTLs are necessary to exert the same degree of immune control over the tumor. However, strong chemotherapy on a patient with lower k_0 values prevents sufficient CTL expansion by rapidly diminishing the memory cell populations. Higher CTL killing rates, although, removed the restriction of this Goldilocks Window and made successful treatment outcomes less sensitive to dosing. While higher chemotherapy doses may lead to larger immune depletion, more efficient CTLs mean that these smaller immune populations still lead to successful treatment outcomes.

In addition, we examined the impact of changing the window duration for immune expansion immediately following each chemotherapy dose. Current literature indicates that immune contraction can begin to occur anywhere from 4 to 8 days after treatmen (8, 14, 17) When these extremes were explored (see Supplementary Fig. S1), there was no significant qualitative difference to our observation of a submaximal optimal dosing range when compared between 4 days (Supplementary Fig. S1A) and 8 days (Supplementary Fig. S1B). While a longer window of immune expansion (Supplementary Fig. S1B) leads to more favorable outcomes for more rapidly growing tumors when treated in the optimal dosing range, the actual presence of this submaximal dosing range does not change. Furthermore, there is almost no difference in the outcomes of patients who are over-treated. This also implicitly addresses our mathematical implementation of a switch via a Heaviside Function. Specifically, while there might be any number of less abrupt and more gradual transitions between immune expansion and immune contraction, our exploration of the dynamics at the extremes of this transition range would give an idea of what the intermediate behaviors due to a smoother transition might cause. That is, our qualitative results would not significantly change with a smoother function.

In a broader exploration of the model's immune parameters, a general trend was observed that a more robust immune response would improve the outcome (Supplementary Figs. S2–S7). For certain model parameters that were more difficult to accurately estimate from the literature, we explored their variation for the default tumor growth rate and a chemotherapy strength of 25%. If the patient had a stronger immune system characterized by lower CTL death rate (δ_E), lower sensitivity to Tregs (c), greater memory cell expansion (γ), regrowth (r_M), and back conversion (ω), the final tumor population was smaller. Furthermore, more robust antitumor immune responses led to greater maximum possible reductions over the range of chemotherapy. In addition, these changes led to expansions of the Goldilocks Window in terms of chemotherapy doses that could achieve tumor reductions.

In short, patient-specific disease and immune biology determines the sensitivity of treatment outcomes to chemotherapy dosing. For rapidly growing tumors, chemotherapy must be maintained in a submaximal Goldilocks Window to optimize drug and immune synergies. However, patient immune biology matters as well, with weaker immune characteristics also leading to a greater necessity to stay within the Goldilocks Window. Importantly, this presents potentially counterintuitive guidance because an initial motivation may suggest that, in a situation where a patient has a weaker immune system, chemotherapy strength should be increased to compensate. However, our model suggests that the lymphodepleting impact of heavy chemotherapy on an already weakened immune system will only worsen outcomes. When confronted with weaker patient immune systems, chemotherapy needs to be maintained within the Goldilocks Window for successful outcomes.

Improvements to therapy outcomes from immunostimulatory vaccines

Patient-specific vaccines have become a recent hallmark in personalized cancer therapy. One of the first to acquire FDA approval was Sipuleucel-T, for treating metastatic castrate resistant prostate cancer (50). Each vaccine is tailored to a specific patient by culturing dendritic cells from patients using a specific tumor antigen. Reinjection into the patient would potentially stimulate a T-cell–mediated antitumor immune response. Three doses were administered in 2-week intervals with significant clinical responses being observed. Vaccination led to a 22% reduction in the relative risk of death, although there was no noticeable decrease in the rate of progression of disease (50). The specific effect on T cells was quantified by looking at T-cell receptor changes in response to vaccination. Certain receptor sequences were enriched, while others were significantly decreased (51), suggesting that the vaccine promoted an antigen-specific immune response against the tumor.

To study the effects and potential synergy of chemotherapy with this method of T-cell stimulation, we simulated a vaccine regime similar to that used for Sipuleucel-T (3 doses, spaced 14 days apart), with different vaccine strengths. Mathematically, this was modeled by modifying the ODEs that govern CTL expansion, without explicitly representing the complex DC-to-T-cell cascade that the vaccine induces. Other models have examined the DC cascade in more detail. For example, the explicit migration of dendritic cells between blood, spleen, and tumor have been modeled via delay-differential equations to better characterize the specific dose timing–dependent responses to therapy (28) For simplicity, here we focus solely on the net effect of the vaccine on T-cell numbers by changing the antigenicity parameter of the tumor, α, from a constant coefficient to a variable, time-dependent function, $\alpha_v(t)$:

$$\alpha_v(t) = \alpha + \upsilon\left(\frac{1}{2}\right)^{\frac{t}{t_{half}}} \tag{H}$$

Total antigenicity is modeled as the result of both the constant, baseline antigenicity of the tumor, α, and an exponentially decaying vaccine-augmented component, υ, which decays with a half-life, $t_{half} = 3$ days, a biologically realistic timespan (52). This model of dynamic antigenicity can be expanded for multiple vaccinations, as used in the clinical protocol (Eq. I).

$$\alpha_v(t) = \alpha + \sum_{n=1}^{n_{vac}} H(t - t_n)\upsilon\left(\frac{1}{2}\right)^{\frac{t-t_n}{t_{half}}} \tag{I}$$

Here, $H(t)$ is again the Heaviside function. The constant n_{vac} represents the total number of vaccine injections and t_n represents the time of the n^{th} vaccination. The ODEs used for the simulation of immune and tumor cell populations are then dependent on the instantaneous current value of $\alpha_v(t)$ throughout the course of simulated therapy.

Here, we explored a range of antigenic increases due to potential patient-to-patient variation in responses to immunostimulatory vaccines. While dendritic cell vaccines like Sipuleucel-T

Published OnlineFirst August 6, 2019; DOI: 10.1158/0008-5472.CAN-18-3712

administer all of the available dendritic cells, responses in individual patients vary in how much the antigenicity is changed. In our range of exploration, though, we found some commonalities in vaccine interaction for chemotherapy.

Results show that vaccine therapy can improve outcomes, but only within a specific range of chemotherapy strengths (Fig. 4). Treatment outcomes improve when a vaccine is used with moderate chemotherapy (Fig. 4A), but for very high chemotherapy doses, the beneficial effects of a vaccine are diminished. As before, the underlying cause for decreasing efficacy is the persistent lymphodepletion due to the chemotherapy. Antigenicity augmentation due to vaccine stimulation is offset by reduced CTL expansion. However, very low-dose chemotherapy poses its own challenges, because with insufficient lymphodepletion, tolerogenic mechanisms and greater Treg recruitment inhibit any CTL response augmented by the vaccine. The immune system remains closer to tumor-tolerized homeostasis, and as a result, vaccine stimulation is mitigated because the immune system is already suppressed. Therefore, the width of the optimal window is not significantly affected by the vaccine because the vaccine has no effect on a highly depleted or tolerized immune system.

Therefore, even with immunostimulatory vaccines, there exists an optimal "Goldilocks" Window. Quantitatively, we define this window to be the region in which a therapy dose can offer at least a 20% reduction in tumor size because this is the necessary amount for disease to become classified as a partial response. In order for there to be this maximized benefit from vaccine application, the chemotherapy regimen must be "just right." Chemotherapy must have sufficient lymphodepletion to resensitize the immune system, but must leave enough immune cells such that vaccine stimulation leads to a large CTL response. Similar to the results of chemotherapy without the vaccine, the specific range of this Goldilocks Window depends upon the initial patient memory cell (M_0) numbers.

We note that the small oscillations observed in the plots (Fig. 4B) are a result of the use of dual growth laws for the tumor. Essentially, giving the vaccine causes the tumor to dip into the faster exponential growth phase at an earlier chemo cycle than when chemo is given alone. Because the chemo cycles are discrete and instantaneous, this generates an effective step function to the response with increasing chemo dose, superimposed on the single-peaked optimal curve; this step function is further rounded by both the smoothing exponent P between the growth laws and the nonlinear interactions between tumor growth and immune response at small tumor sizes.

Impact of variation in immune support

Chemotherapeutic lymphodepletion in the clinical setting can pose a serious threat to the safety of the patient through neutropenia (53), which commonly leads to dose reductions and disruptions to the standard schedule of therapy for patients. Consequently, multiple tools have been developed to help mitigate the effects of chemotherapy on the immune system. For example, it was recognized that dexamethasone treatment before carboplatin and gemcitabine could not only increase chemotherapy efficacy, but also reduce the lymphodepleting effects by preventing uptake in the spleen and bone marrow (54). In contrast, other aspects of cancer therapy can potentially hamper CTL responses to tumor insults. For example, G-CSF application has been shown to reduce CTL

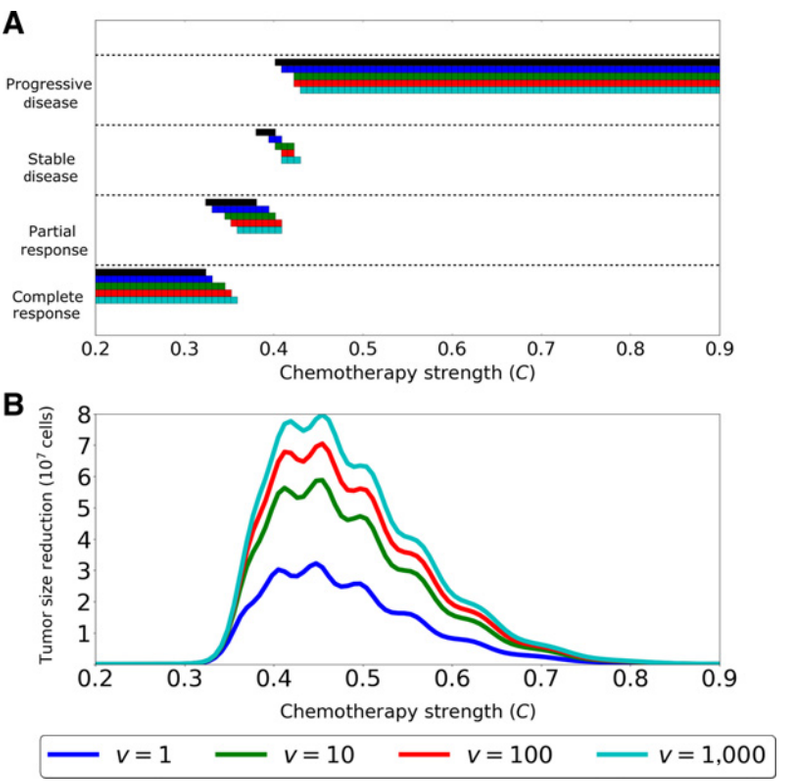

Figure 4.

Improvements in tumor reduction due to vaccine application. **A,** The RECIST responses achieved for different vaccine strengths and chemotherapy strengths, with black being the nonvaccine baseline. Vaccine strengths (***v***) are 1 (blue), 10 (green), 100 (red), 1000 (light blue). Larger vaccine strengths lead to more successful RECIST responses for stronger chemotherapy doses. When looking at the absolute number of improvement in cellular reduction (**B**), a window of optimal chemotherapy ranges appears. Only when chemotherapy is in this range can vaccines provide a significant additional benefit.

Published OnlineFirst August 6, 2019; DOI: 10.1158/0008-5472.CAN-18-3712

activation and could conceivably impede the impact of lymphodepletion as a break from immune tolerance (55, 56). More generally, however, the broader impact of immune system augmentation or suppression during therapy remains unexamined.

To examine the effect of attenuated or augmented lymphodepletion on therapy outcome, we allowed for variable chemotherapeutic toxicity to immune populations, as compared with the tumor population. Mathematically, this simply means modifying the chemotherapy dose by a scaling factor h. The effect of chemotherapy on immune cell populations at a given treatment time is:

$$I_1 = I_0(1 - hC) \quad \text{(J)}$$

where I_1 is the immunologic population size after application of chemotherapy, I_0 is the population size before therapy, and $0 < C < 1$ is the dose strength. The specific numerical range in which h falls represents either attenuated or augmented chemotherapeutic toxicity. For values of $0 < h < 1$, this represents an attenuated toxicity on the immune system relative to the toxicity on the tumor. In contrast, values of $h > 1$ represent higher toxicity on patient immune populations than on the tumor. This could be due to patient-dependent increased sensitivity to chemotherapy. The maximum possible reduction of cells by chemotherapy when modified by immune support is 100%. This leads to the resulting condition that $hC < 1$. For our *in silico* therapies, h was varied across the allowable ranges for three different strengths of chemotherapy. Values of C were chosen to represent lower ($C = 0.25$), middle ($C = 0.6$), and higher ($C = 0.9$) dose chemotherapy (Fig. 5A).

Interestingly, the results suggest that immune-supporting combination therapy has essentially no benefit when given with low-dose chemotherapy. As shown in Fig. 5, similar tumor reduction occurred for a wide range of values of h around $h = 1$. Furthermore, outcomes were worse when h was very low or very high. In situations where it was very low, final tumor sizes were large because a lack of lymphodepletion did not sufficiently break immune tolerance. In contrast, for larger h values, there was overdepletion that prevented an effective immune response despite significant tolerance breaking.

In contrast, high-dose chemotherapy saw treatment failure or success highly dependent upon the amount of immune support. Similar to low-dose therapy, a small value of h that mitigated the depleting effects of chemotherapy led to the best possible outcomes in terms of tumor shrinkage. Final tumor sizes were, in fact, multiple orders of magnitude lower than was possible with low-dose chemotherapy. As h increased (representing less toxicity mitigation) treatment outcomes rapidly worsened. The transition value h^*, where the clinical outcome rapidly shifts, indicates a threshold effect with regard to immune support. For high chemotherapy doses, immune support treatments must have a significantly large mitigation ($h < h^*$) of immunodepletion in order for successful treatment responses to occur. The position of this inflection point is influenced by the strength of the patient immune system to begin with. In expanded parameter analyses, the strength or weakness of the simulated patient's immune system led to changes in the upper bound of the Goldilocks Window (Supplementary Figs. S2–S7).

The moderate strength chemotherapy regimen yielded only partial benefits of either extreme. The greatest tumor reduction

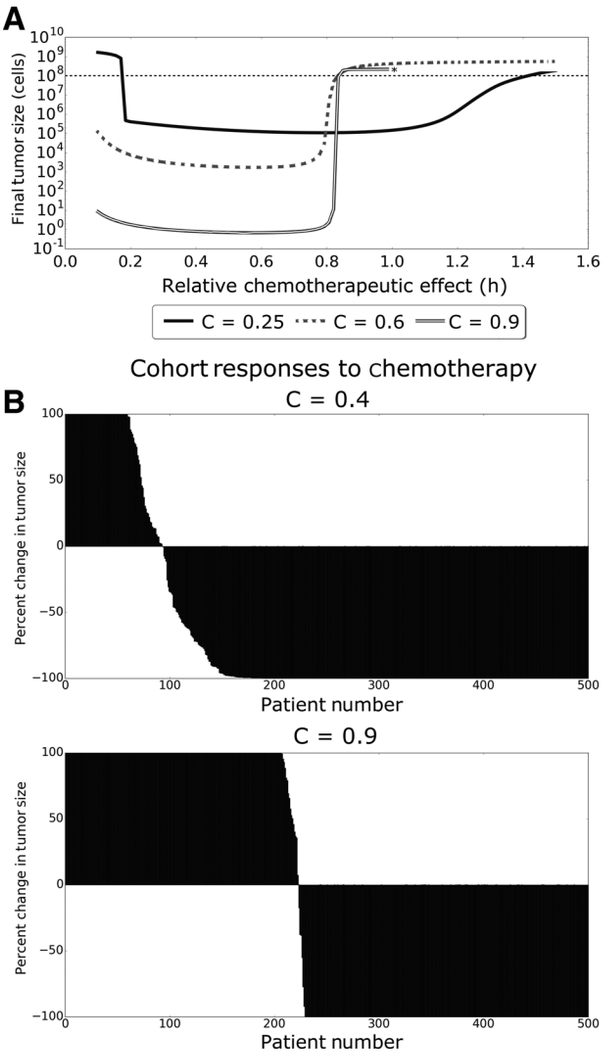

Figure 5.
Therapeutic effects of differential response to immune prophylactics. **A,** Final tumor sizes are shown for three different chemotherapy regimes ($C = 0.25$, black curve; $C = 0.6$, dotted curve; $C = 0.9$, outlined curve) for a range of immune modifier efficacies (h). The asterisk denotes that simulations were only run up to this h value for the highest dose chemotherapy. The dotted line represents the tumor size at the start of therapy. **B,** Cohorts were treated with these differing regimes of high and low chemotherapy, showing significant differences in the proportion of successful versus unsuccessful responders.

possible, with immune support, yielded tumors that were smaller than those achievable with low-dose chemotherapy. However, these tumors were still multiple orders of magnitude larger than those achievable with high-dose chemotherapy. For treatment failure at lower immune support ($h > h^*$), tumor sizes were actually larger than when high dose chemotherapy failed.

Clinically, the results suggest that chemotherapy dose strength can be used to mitigate uncertainty regarding the amount of immune support a certain treatment will give to a specific patient. Low-dose therapy offers a wide range of potential immune support in which treatment can successfully

Published OnlineFirst August 6, 2019; DOI: 10.1158/0008-5472.CAN-18-3712

reduce tumor sizes. The disadvantage is that the maximum tumor size reduction still leaves larger tumors than are possible using higher doses of chemotherapy. While our model has not analyzed this, a potential impact is that larger tumor sizes could lead to more heterogeneous populations and thus lead to a higher likelihood of resistant or metastatic populations. However, higher doses have a narrower range of immune support in which they are successful. Chemotherapy can be balanced, then, against how certain the clinician is of the benefit that G-CSF (or other immune supporting drug) will give. For patients where there is high certainty of a significant benefit due to the drug, high-dose therapy is optimal. In contrast, lower dosing should be used when the drug may have lower or variable efficacy.

Finally, we sought to investigate how variation in the effectiveness of these immune adjuvants might impact treatment outcomes in a group of patients. Chemotherapy treatment leads to a wide range of responses, both successful and unsuccessful, across multiple types of cancer (47). This variation has been attributed to disease variation, patient variation, and interactions between the two. However, less attention has been given to variable patient responses to secondary drugs, such as G-CSF, and how they impact therapy. Patient responses to these secondary drugs are currently poorly measured and could have significant implications for therapy outcomes.

To better explore the effect of variable patient responses to immune support drugs, cohorts of 500 patients were randomly generated from a normal distribution with a mean immune support response value of $h = 0.8$ and variance of 0.2. These values were chosen to center the distribution around the model-derived threshold value $h^* = 0.8$. While not directly describing patient responses to immune support drugs, a normal distribution for selection was chosen due to the fact that immune cell counts have been found to be normally distributed in population cohorts (57).

Similar to our previous investigations, cohorts were then subjected to regimens of low ($C = 0.4$) and high ($C = 0.8$) chemotherapy strengths (Fig. 5B). Percent changes in tumor size after therapy were displayed for each individual patient in the cohort to generate a waterfall plot. In doing so, we used our model to simulate cohort responses as is commonly measured in aggregated studies of patient data (47). The waterfall plots (Fig. 5) illustrate that chemotherapy strength can significantly change the proportion of successfully responding patients in a population with variable responses to immune prophylactics. This is significant because the proportion of successful responses is often an important criterion for judging therapeutic efficacy. The simulated waterfall plots show how clinical outcomes could not only be the result of therapy, but also due to inherent immune variation within the cohort.

Discussion

A major barrier to success for immunotherapy in cancer is tolerogenic mechanisms that reduce the immune response to tumor antigen (4, 7, 58). A potential solution has come from observations that lymphodepletion stimulates homeostatic proliferation in the immune system that can transiently restore an immune response. This has led to increasing efforts to selectively apply chemotherapy to improve outcomes from immunotherapy (59).

To better understand this potential synergy, we constructed a mathematical model to frame these complex dynamics and identify critical parameters that govern the clinical outcomes. Our studies focused on three clinically observed dynamics of immunodepletion, immunostimulatory vaccination, and immunosupportive prophylactics. With regard to immunodepletion, we demonstrated that chemotherapy results in a trade-off. At very high doses, chemotherapy has a maximal cytotoxic effect on the tumor but also maximally depletes T cells such that no effective CTL response can be mounted despite the transient loss of tolerance during reexpansion of the immune cells after completion of chemotherapy. Similarly, low doses of chemotherapy are insufficient to produce the post-treatment immune cell expansion that is necessary for reversal of immune tolerance.

Importantly, however, we find there is a Goldilocks Window of chemotherapy doses in which lymphodepletion causes adequate immune resensitization, but does not impose an overly large recovery burden. This window is governed by the patient-specific quantity of memory T cells so that larger pretreatment T-cell populations allow more favorable outcomes with higher doses of chemotherapy. In contrast, fewer pretreatment CTLs can limit the immune response even in the Goldilocks window of chemotherapy. Thus, there is a necessary "minimum efficacy" of CTLs for successful stimulation of immune response by chemotherapy. Below this threshold of immune activity, the benefit of chemotherapy is almost solely dependent on its inherent cytotoxicity (Fig. 6).

Our model also provides insight into the potential effects of variation in the tumor growth rate. In slower growing tumors, chemotherapy alone can be sufficient to achieve optimal treatment response. Treatment of faster growing tumors, however, is best when the chemotherapy is administered to enhance the immune response. Unfortunately, if the pretreatment population of CTLs is small, we find chemotherapy for rapidly growing tumors will be ineffective if it is both highly lymphodepleting

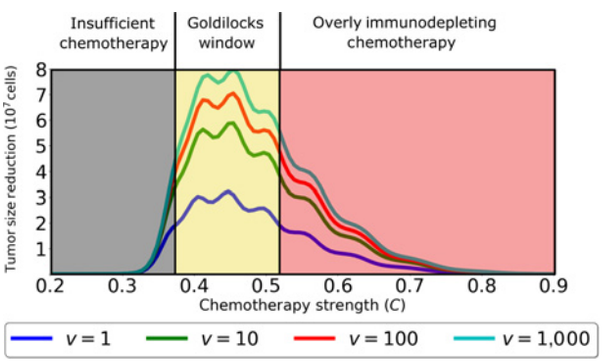

Figure 6.

A diagram explaining tumor outcomes at varying chemotherapy strengths and immune support doses. If therapy is too weak, then immune stimulation cannot be maximally effective and direct chemotherapy-mediated tumor cell death is also low. This yields a suboptimal tumor reduction. When chemotherapy is too strong, there may be more tumor cell death due to the drug, but insufficient immune activation due to overdepletion of T cells. There is a moderate dose, however, that represents a Goldilocks Window of maximizing both T-cell activation as well as drug-induced tumor cell death. This range of dosing provides at least a 20% reduction in tumor size (relative to the initial tumor size of 10^8 cells).

Published OnlineFirst August 6, 2019; DOI: 10.1158/0008-5472.CAN-18-3712

and insufficiently cytotoxic to significantly reduce tumor growth. Assessing the clinical importance of this question is challenging because it remains unclear from the literature as to the actual size of the population of tumor-specific T cells that are present during treatment. In spite of these difficulties, the impact and existence of antitumor immunity has been bolstered by recent immunotherapies that act to remove inhibitions to T-cell action (60).

Chemotherapy is increasingly being used in concert with vaccines to help stimulate the patient immune system. We investigated the interactions between vaccines and lymphodepletion and found that, as before, there is a window of chemotherapy ranges in which vaccines can improve outcomes versus chemotherapy alone. At very high doses, however, the resulting lymphodepletion substantially reduces benefits of immune stimulation by vaccination. More broadly, other novel immunotherapies could also potentially be hampered by overdepletion of the immune system.

To further investigate the potential impact of this interaction, we modeled the effect of differential responses to immune prophylactics. G-CSF and other drugs have become common recourses in chemotherapy for mitigating the immunodepletion effects on patients (61). However, recent studies have suggested that T cell response is hampered by G-CSF administration (55). While G-CSF may help prevent neutropenia and cytopenia for patients, it may impede the ability of retolerized T cells to mount an antitumor response. In addition, responses to prophylactics are not constant but the significance of this variation remains relatively uninvestigated. Our model suggests that interpatient variation in prophylactic response can lead to drastically different outcomes for the same dosing of chemotherapy. Across larger samples, this variation can further interact with chemotherapy to be a significant determinant of whether the chemotherapy dose leads to more success or failure across a range of patients.

In the clinical literature, our model results cautioning about balancing chemotherapy and immunogenic effects has been echoed in multiple situations. Previous studies have explored the mechanisms of action in mAb-based treatments including targeting of HER2 (62, 63). When quantifying the impact of antibody-dependent cytotoxicity-mediated by CTLs, it was noted that addition of paclitaxel reduced the lasting impact of the immune response generated against the tumor. While in the short term, higher doses of chemotherapeutic agents could induce larger tumor reductions, mice that were given both antigen and large chemotherapy doses were more susceptible to tumor rechallenge. Similarly, in radiotherapy it has been found that CTL priming occurs due to antigen-dependent cell death (64). However, the addition of even a small amount of paclitaxel was found to induce a significant reduction in CTL numbers. Adjuvant chemotherapy regimens were found to significantly abrogate the immunogenic benefits of radiotherapy-induced immune responses, while immunotherapies increased the efficacies. This result is also significant because it implicitly addresses whether our results might hold when antigen increase, due to cell death, is accounted for. In this mouse model, even with tumor-cell death–mediated antibodies, the loss of T cells leads to a worse overall outcome (64). This presents a natural extension of our framework to be applied to a specific disease and chemotherapy dosing setting. While we created a general model of chemotherapy, there may be interesting dynamics unique to individual cancers that could be explored. It would also allow the employment of more complex pharmacodynamics modeling for specific treatment regimens.

In conclusion, our results suggest opportunities to increase the efficacy of immunotherapy with precise application of chemotherapy. Our model affirms the importance of CTL and memory T-cell expansion following chemotherapy to reduce immune tolerance to tumor antigens. However, we demonstrate that optimal chemotherapy requires identification of a Goldilocks Window in which treatment can both induce cytotoxic effects in the tumor and enhance the immune response to tumor antigens. Identifying optimal strategies for chemotherapy in each patient will likely benefit from the application of mathematical models that are parameterized by patient data pretreatment to generate an optimal treatment strategy for that patient. Importantly, these predicted strategies would most likely need to change as patient responses diverge from those predicted, leading to an iterative loop of "predict-apply-refine." With the growing drive toward precision medicine, we believe that mathematical models are critical for the future of truly personalized therapy, where no two patients will receive the same therapeutic regimen, and where treatments adapt a change based on patient responses. The model presented here is a step toward describing the complex landscape of treatment decisions regarding dosing and combination of different therapies, and we have shown how these decisions can be sensitive to patient-specific parameters and guide clinical intuition.

Disclosure of Potential Conflicts of Interest

No potential conflicts of interest were disclosed.

Authors' Contributions

Conception and design: D.S. Park, M. Robertson-Tessi, K.A. Luddy, P.K. Maini, A.R.A. Anderson

Development of methodology: D.S. Park, M. Robertson-Tessi, K.A. Luddy, P.K. Maini, A.R.A. Anderson

Acquisition of data (provided animals, acquired and managed patients, provided facilities, etc.): D.S. Park

Analysis and interpretation of data (e.g., statistical analysis, biostatistics, computational analysis): D.S. Park, M. Robertson-Tessi, K.A. Luddy, P.K. Maini, M.B. Bonsall

Writing, review, and/or revision of the manuscript: D.S. Park, M. Robertson-Tessi, K.A. Luddy, P.K. Maini, M.B. Bonsall, R.A. Gatenby, A.R.A. Anderson

Administrative, technical, or material support (i.e., reporting or organizing data, constructing databases): D.S. Park

Study supervision: M. Robertson-Tessi, P.K. Maini, A.R.A. Anderson

Other (source code maintenance): D.S. Park

Acknowledgments

D. Park was supported by a 2014 Marshall Scholarship from the Marshall Aid Commemoration Commission of Great Britain. A.R.A. Anderson, R.A. Gatenby, M. Robertson-Tessi, and K. A. Luddy were supported by a Physical Sciences-Oncology Center grant from the National Cancer Institute of the United States of America (grant number 1U54CA193489) and the Center of Excellence for Evolutionary Therapy at H. Lee Moffitt Cancer Center and Research Institute.

The costs of publication of this article were defrayed in part by the payment of page charges. This article must therefore be hereby marked *advertisement* in accordance with 18 U.S.C. Section 1734 solely to indicate this fact.

Received December 12, 2018; revised May 20, 2019; accepted August 1, 2019; published first August 6, 2019.

References

1. Xing Y, Hongquist KA. T-cell tolerance: central and peripheral. Cold Spring Harb Perspect Biol 2012;4:6.
2. Nurieva R, Wang J, Sahoo A. T-cell tolerance in cancer. Immunotherapy 2013;5:513–31.
3. Corthay A. How do regulatory T cells work?. Scand J Immunol 2009;70: 326–36.
4. Tanaka A, Sakaguchi S. Regulatory T cells in cancer immunotherapy. Cell Res 2017;27:109–18.
5. Thomas D, Massgue J. TGF-beta directly targets cytotoxic T cell functions during tumor evasion of immune surveillance. Cancer Cell 2005;8: 369–80.
6. McKarns S, Schwarz R. Distinct effects of TGF-beta 1 on CD4(+) and CD8(+) T cell survival, division, and IL-2 production: a role for T cell intrinsic Smad3. J Immunol 2005;174:2071–83.
7. Takeuchi Y, Nishikawa H. Roles of regulatory T cells in cancer immunity. Int Immunol 2016;28:401–9.
8. Zheng Y, Dou Y, Duan L, Cong C, Gao A, Lai Q, et al. Using chemo-drugs or irradiation to break immune tolerance and facilitate immunotherapy in solid cancer. Cell Immunol 2015;294:54–9.
9. Cook AM, Lesterhuis WJ, Nowak AK, Lake RA. Chemotherapy and immunotherapy: mapping the road ahead. Curr Opin Immunol 2016;39:23–9.
10. Hodge JW, Garnett CT, Farsaci B, Palena C, Tsang K-Y, Ferrone S, et al. Chemotherapy-induced immunogenic modulation of tumor cells enhances killing by cytotoxic T lymphocytes and is distinct from immunogenic cell death. Int J Cancer 2013;133:624–36.
11. Bracci L, Schiavoni G, Sistigu A, Belardelli F. Immune-based mechanisms of cytotoxic chemotherapy: implications for the design of novel and rationale-based combined treatments against cancer. Cell Death Differ 2014; 21:15–25.
12. Tchao NK, Turka LA. Lymphodepletion and homeostatic proliferation: implications for transplantation. Am J Transplant 2012;12:1079–90.
13. Wrzensinski C, Paulos C, Kaiser A, Muranski P, Palmer D, Gattinoni L, et al. Increased intensity lymphodepletion enhances tumor treatment efficacy of adoptively transferred tumor-specific T cells. J Immunother 2010;33:1–7.
14. Gameiro SR, Caballero JA, Higgins JP, Apelian D, Hodge JW. Exploitation of differential homeostatic proliferation of T-cell subsets following chemotherapy to enhance the efficacy of vaccine-mediated antitumor responses. Cancer Immunol Immunother 2011;60:1227–42.
15. Marco MR, Dons EM, van der Windt DJ, Bhama JK, Lu LT, Zahorchak AF, et al. Post-transplant repopulation of naïve and memory T cells in blood and lymphoid tissue after alemtuzumab-mediated depletion in heart-transplanted cynomolgus monkeys. Transpl Immunol. 2013;29:88–98.
16. Althaus C, Ganusov V, De Boer R. Dynamics of CD8(+) T cell responses during acute and chronic lymphocytic choriomeningitis. J Immunol 2007; 17:2944–51.
17. Schwarz RH. Historical Overview of Immunological Tolerance. Cold Spring Harb Perspect Biol 2012;4:4.
18. Alizadeh D, Larmonier N. Chemotherapeutic targeting of cancer-induced immunosuppressive cells. Cancer Res 2014;74:2663–8.
19. Lutsiak MEC. Inhibition of CD425 T regulatory cell function implicated in enhanced immune response by low-dose cyclophosphamide. Blood 2005; 105:2862–8.
20. Dummer W, Niethammer AG, Baccala R, Lawson BR, Wagner N, Reisfeld RA, et al. T cell homeostatic proliferation elicits effective antitumor autoimmunity. J Clin Invest 2002;110:185–92.
21. Schietinger A, Delrow JJ, Basom RS, Blattman JN, Greenberg PD. Rescued tolerant CD8 T cells are preprogrammed to reestablish the tolerant state. Science 2012;335:723–7.
22. Kline J, Brown IE, Zha YY, Blank C, Strickler J, Wouters H, et al. Homeostatic proliferation plus regulatory T-cell depletion promotes potent rejection of B16 melanoma. Clin Cancer Res 2008;14:3156–67.
23. Meir H, Nout RA, Welters MJP, Loof NM, Kam ML, Ham JJ, et al. Impact of (chemo)radiotherapy on immune cell composition and function in cervical cancer patients. OncoImmunology 2017;6:e1267095.
24. Wilkie KP, Hahnfeldt P. Modeling the dichotomy of the immune response to cancer: cytotoxic effects and tumor-promoting inflammation. Bull Math Biol 2017;79:1426–48.
25. Lai X, Friedman A. Combination therapy of cancer with cancer vaccine and immune checkpoint inhibitors: a mathematical model. PLoS One 2017; 12:e0178479.
26. Eftimie R, Dushoff J, Bridle BW, Bramson JL, Earn DJD. Multi-stability and multi-instability phenomena in a mathematical model of tumor-immune-virus interactions. Bull Math Biol 2011;73:2932–61.
27. Ledzewicz U, Naghnaeian M, Schättler H. Optimal response to chemotherapy for a mathematical model of tumor–immune dynamics. J Math Biol 2011;64:557–77.
28. DePillis L, Gallegos A, Radunskaya A. A model of dendritic cell therapy for melanoma. Front Oncol 2013;3. doi: 10.3389/fonc.2013.00056.
29. Robertson-Tessi M, El-Kareh A, Goriely A. A mathematical model of tumor-immune interactions. J Theor Biol 2012;294:56–73.
30. De Pillis LG, Radunskaya A. The dynamics of an optimally controlled tumor model: a case study. Math Comput Modell 2003;37:1221–44.
31. Hinow P, Gerlee P, McCawley LJ, Quaranta V, Ciobanu M, Wang S, et al. A spatial model of tumor-host interaction: application of chemotherapy. Math Biosci Eng 2009;7:521–46.
32. Hamis S, Powathil GG, Chaplain MAJ. Blackboard to bedside: a mathematical modeling bottom-up approach toward personalized cancer treatments. JCO Clin Cancer Inform 2019;3:1–11.
33. Cheung KP, Yang E, Goldrath AW. Memory-Like CD8 T cells generated during homeostatic proliferation defer to antigen-experienced memory cells. J Immunol 2009;183:3364–72.
34. Diefenbach A, Jensen E, Jamieson A, Raulet D. Rae1 and H60 ligands of the NKG2D receptor stimulate tumour immunity. Nature 2001;413:165–71.
35. Halle S, Keyser KA, Stahl FR, Busche A, Marquardt A, Zheng X, et al. *In vivo* killing capacity of cytotoxic T cells is limited and involves dynamic interactions and T cell cooperativity. Immunity 2016;44:233–45.
36. Gattinoni L, Finkelstein S, Klebanoff C, Antony P, Palmer D, Spess P. Removal of homeostatic cytokine sinks by lymphodepletion enhances the efficacy of adoptively transferred tumor-specific CD8(+) T cells. J Exp Med 2005;202:907–12.
37. Sakaguchi S, Wing K, Onishi Y, Prieto-Martin P, Yamaguchi T. Regulatory T cells: how do they suppress immune responses?. Int Immunol 2009;21: 1105–11.
38. Cui W, Kaech S. Generation of effector CD8+T cells and their conversion to memory T cells. Immunol Rev 2010;236:151–66.
39. Vignali DAA, Collison LWWCJ. How regulatory T cells work. Nat Rev Immunol 2008;8:523–32.
40. Bains I, Antia R, Callard R, Yates A. Quantifying the development of the peripheral naive CD4(+) T-cell pool in humans. Blood 2009;113:5480–7.
41. Richert-Spuhler LE, Lund JM. The immune fulcrum: regulatory T cells tip the balance between pro- and anti-inflammatory outcomes upon infection. Prog Mol Biol Transl Sci 2015;136:217–43.
42. Antony P, Piccirillo C, Akpinarli A, Finkelstein S, Speiss P, Surman D, et al. CD8+ T cell immunity against a tumor/self-antigen is augmented by CD4+ T helper cells and hindered by naturally occurring T regulatory cells. J Immunol 2005;5:2591–601.
43. Lythe G, Callard RE, Hoare RL, Molina-Paris C. How many TCR clonotypes does a body maintain?. J Theor Biol:2016;389:214–24.
44. Kufe DW, Major PP. 5-fluorouracil incorporation into human breast carcinoma RNA correlates with cytotoxicity. J Biol Chem 1981;256: 9802–5.
45. Arancia G, Calcabrini A, Meschini S, Molinari A. Intracellular distribution of anthracyclines in drug resistant cells. Cytotechnology 1998;27:95–111.
46. Hao J, Madigan M, Khatri A, Power C, Hung T, Beretov J, et al. In vitro and in vivo prostate cancer metastasis and chemoresistance can be modulated by expression of either CD44 or CD147. PLoS One 2012;7:e40716.
47. Jain R, Lee J, Ng C, Hong D, Gong J, Naing A, et al. Change in tumor size by RECIST correlates linearly with overall survival in phase I oncology studies. J Clin Oncol 2012;30:2684–90.
48. Arstila T, Casrouge A, Baron V, Even J, Kanellopoulos J, Kourilsky P. A direct estimate of the human alphabeta T cell receptor diversity. Science 1999; 286:958–61.
49. Robertson-Tessi M, Gillies R, Gatenby R, Anderson A. Impact of metabolic heterogeneity on tumor growth, invasion, and treatment outcomes. Cancer Res 2015;75:1567–79.
50. Plosker G. Sipuleucel-T in metastatic castration-resistant prostate cancer. Drugs 2011;71:101–8.
51. Sheikh N, Cham J, Zhang L, DeVries T, Letarte S, Pufnock J, et al. Clonotypic diversification of intratumoral T cells following sipuleucel-T treatment in prostate cancer subjects. Cancer Res 2016;76:3711–8.

Published OnlineFirst August 6, 2019; DOI: 10.1158/0008-5472.CAN-18-3712

52. Merad M, Manz M. Dendritic cell homeostasis. Blood 2009;113: 3418–27.
53. Crawford J, Dale D, Lyman G. Chemotherapy-induced neutropenia - Risks, consequences, and new directions for its management. Cancer 2004;100: 228–37.
54. Wang H, Li M, Rinehart J, Zhang R. Dexamethasone as a chemoprotectant in cancer chemotherapy: hematoprotective effects and altered pharmacokinetics and tissue distribution of carboplatin and gemcitabine. Cancer Chemother Pharmacol 2004;53:459–67.
55. Bunse CE, Tischer S, Lahrberg J, Oelke M, Figueiredo C, Blasczyk R, Eiz-Vesper B. Granulocyte colonystimulating factor impairs CD8+ T cell functionality by interfering with central activation elements. Clin Exp Immunol 2016;185:107–18.
56. Freyer G, Jovenin N, Yazbek G, Villanueva C, Hussain A, Berthune A, et al. Granocyte-colony stimulating factor (G-CSF) has significant efficacy as secondary prophylaxis of chemotherapy-induced neutropenia in patients with solid tumors. Anticancer Res 2013;33:301–7.
57. Lugada ES, Mermin J, Kaharuza F, Ulvestad E, Were W, Lageland N, et al. Population-based hematologic and immunologic reference values for a healthy ugandan population. Clin Diagn Lab Immunol 2004;11:29–34.
58. Kim R, Emi M, Tanabe K. Cancer immunoediting from immune surveillance to immune escape. Immunology 2007;121:1–14.
59. Makkouk A, Weiner G. Cancer immunotherapy and breaking immune tolerance: new approaches to an old challenge. Cancer Res 2015;75:5–10.
60. Guo H, Tsung K. Tumor reductive therapies and antitumor immunity. Oncotarget 2017;8:55736–49.
61. Mehta HM, Malandra MJCS. G-CSF and GM-CSF in Neutropenia. J Immunol 2015;195:1341–9.
62. Park S, Jiang Z, Mortenson ED, Deng L, Radkevich-Brown O, Yang X, et al. The therapeutic effect of anti-HER2/neu antibody depends on both innate and adaptive immunity. Cancer Cell 2010;18:160–70.
63. Ferris RL, Jaffee EM, Ferrone S. Tumor antigen–targeted, monoclonal antibody–based immunotherapy: clinical response, cellular immunity, and immunoescape. J Clin Oncol 2010;28:4390–9.
64. Lee Y, Auh SL, Wang Y, Burnette B, Wang Y, Meng Y, et al. Therapeutic effects of ablative radiation on local tumor require CD8+ T cells: changing strategies for cancer treatment. Blood 2009;114:589–95.

Cancer Research
The Journal of Cancer Research (1916–1930) | The American Journal of Cancer (1931–1940)

AACR American Association for Cancer Research

The Goldilocks Window of Personalized Chemotherapy: Getting the Immune Response Just Right

Derek S. Park, Mark Robertson-Tessi, Kimberly A. Luddy, et al.

Cancer Res 2019;79:5302-5315. Published OnlineFirst August 6, 2019.